Macromolecules
ARTICLE

Macromolecules **2010**, *43*, 7033–7040 **7033**
DOI: 10.1021/ma100983p

Reversible Interpolyelectrolyte Shell Cross-Linked Micelles from pH/Salt-Responsive Diblock Copolymers Synthesized via RAFT in Aqueous Solution†

Matthew G. Kellum,‡ Adam E. Smith,‡ Stacey Kirkland York,‡ and Charles L. McCormick*,‡,§

‡*Department of Polymer Science and* §*Department of Chemistry and Biochemistry, University of Southern Mississippi, Hattiesburg, Mississippi 39406*

Received May 11, 2010; Revised Manuscript Received July 15, 2010

ABSTRACT: Herein we report the synthesis and characterization of a series of pH reversible shell cross-linked micelles. A series of novel pH/salt-responsive block copolymers of poly(sodium 2-acrylamido-2-methyl-1-propanesulfonate-*block*-*N*-acryloyl-L-alanine) (P(AMPS-*b*-AAL)) were synthesized utilizing aqueous reversible addition−fragmentation chain transfer (RAFT) polymerization. Micellization of P(AMPS-*b*-AAL) is induced by rendering the PAAL block hydrophobic through protonation of the carboxylic acid (pH 1−3). The pH at which micelle formation occurs and the hydrodynamic diameters of the resultant micelles are dictated by block copolymer composition and electrolyte concentration. The anionic PAMPS micelle shells were subsequently cross-linked with a RAFT synthesized cationic homopolymer of either poly(*N*-[3-(dimethylamino)-propyl]acrylamide) (PDMAPA, pK_a = 8.5) or poly(*N*,*N*-dimethylaminoethyl methacrylate) (PDMAEMA, pK_a = 7.3). Upon deprotonation of the PAAL block, these cross-linked micelles swell but remain stable and intact. Significantly, the reversibility of the cross-linking was determined to be tunable by utilizing the different cationic homopolymers for cross-linking. This was demonstrated by increasing the pH above the pK_a of the cationic homopolymer cross-linker, resulting in deprotonation of the cationic cross-linker and dissociation of the cross-linked micelles.

Introduction

Recently, a great deal of interest has been focused on the synthesis of well-defined, water-soluble block copolymers capable of self-assembling in response to external stimuli. These polymers typically contain a permanently hydrophilic block and a responsive block which upon application of an external stimulus (i.e., temperature, pH, or electrolyte concentration) is rendered hydrophobic. Upon conversion to a hydrophilic−hydrophobic copolymer, self-assembly into higher order structures such as micelles is possible.[1−6] The ability to control the assembly/disassembly process through environmental cues makes these materials attractive candidates for controlled release applications in which hydrophobic agents are loaded into the core of the structure and subsequently carried until exposed to an external stimulus.[7−21] However, practical applications remain limited due to dilution effects, specifically the disassembly of micelles into unimers as the concentration of polymer falls below the critical micelle concentration.

In order to circumvent dilution effects, researchers have developed a number of methods to either permanently or reversibly cross-link the micelles. In the seminal report on covalent shell cross-linked (SCL) micelles, Wooley and co-workers utilized free radical chemistry to cross-link pendent vinyl groups within the shells of micellar assemblies.[22] Subsequently, numerous shell cross-linking methods have been developed including UV-induced coupling of cinnamoyl groups,[23−25] carbodiimide coupling,[7,26,27] quaternization of amines using 1,2-bis(2-iodoethoxy)ethane,[28−30] cross-linking pendent hydroxyls with divinyl sulfone,[31,32] click chemistry,[33] and multivalent Au ligation through *in situ* reduction.[34,35] Recently, our group reported the facile formation of SCL micelles and reversible SCL micelles utilizing a reaction between activated esters and diamines.[36−39] Briefly, a disulfide-containing diamine (cysteamine) was reacted with activated esters within a micellar shell. By introducing reducing/oxidizing agents, the cross-links could be formed or broken. Since initial reports on shell cross-linking, a number of alternate cross-linking procedures have been introduced and are described in a review by Armes et al.[40]

Although advantageous, many of these cross-linking techniques are limited by low reaction efficiency, reagent insolubility, irreversibility, and extensive purification techniques to remove small molecule byproducts. An alternate approach involves the careful design of polymeric micelles containing charged segments for complexation with oppositely charged polymers to form interpolyelectrolyte complexed micelles.[41] This technique provides many advantages over traditional cross-linking reactions including near instantaneous cross-linking, solvent selection (aqueous environment), lack of byproducts, and reversibility in the presence of added electrolytes. Previously, our group designed both temperature[3,42] and pH[43] responsive systems capable of forming these interpolyelectrolyte complex micelles and demonstrated their reversibility with added electrolytes. Although reversible, a high salt concentration (> 1 M) is required to disrupt these cross-linked micelles rendering them impractical for use as drug delivery vehicles. In order to circumvent these deficiencies, we have designed a novel micelle-forming, pH-responsive block copolymer system cross-linked via interpolyelectrolyte complexation in which the cross-linking is reversibly induced by a change in solution pH. Even more importantly, we demonstrate that the extent of pH-induced dissociation of shell cross-linked micelles can be altered by simply changing the cationic homopolymer used to form the interpolyelectrolyte complex.

Herein, we report the strategic design of pH-responsive, micelle-forming block copolymers which contain an anionically charged corona and an insoluble protonated core at low pH. The

† Paper number 148 in a series on Water-Soluble Polymers.

*Corresponding author. E-mail: Charles.McCormick@usm.edu.

Published on Web 07/30/2010

block copolymers which comprise the micelles were synthesized via aqueous reversible addition−fragmentation chain transfer (RAFT) polymerization and consist of a hydrophilic, anionically charged poly(sodium 2-acrylamido-2-methyl-1-propanesulfonate) (PAMPS) block and a pH-responsive poly(*N*-acryloyl-L-alanine) (PAAL) block. These block copolymers undergo a reversible unimer-to-micelle transition upon lowering the solution pH. The micelles can be cross-linked via interpolyelectrolyte complexation utilizing the anionic PAMPS shell and a cationic homopolymer, in the current case either protonated poly(*N*-[3-(dimethylamino)-propyl]acrylamide) (PDMAPA) or poly(*N*,*N*-dimethylaminoethyl methacrylate) (PDMAEMA). The pH reversibility of these systems is demonstrated by increasing the solution pH to deprotonate the polycation cross-linker, resulting in dissociation of the cross-linked micelles to their respective water-soluble unimer components.

Experimental Section

Materials. All reagents were purchased from Aldrich at the highest purity available and used as received unless otherwise stated. 4-Cyanopentanoic acid dithiobenzoate (CTP) was synthesized according to literature procedures.[44] 4,4′-Azobis-(4-cyanopentanoic acid) (V-501) was donated by Wako Chemicals and was recrystallized twice from methanol before use. DMAPA was purchased from TCI and vacuum-distilled prior to use. AAL was synthesized according to literature procedures.[3] The synthesis of poly(*N*,*N*-dimethylaminoethyl methacrylate) (PDMAEMA) was previously reported.[35]

Instrumentation. Block copolymers of P(AMPS$_n$-*b*-AAL$_m$) were analyzed by aqueous size exclusion chromatography (ASEC) using an aqueous eluent of 20%/80% acetonitrile/0.05 M Na_2SO_4(aq). A flow rate of 0.3 mL/min, TOSOH Biosciences TSK-GEL columns (G3000 PWXL, $<50\,000$ g mol^{-1}, 200 Å) and (G4000PWXL, 2000−300 000 g mol^{-1}, 500 Å), Wyatt Optilab DSP interferometric refractometer, and a Wyatt DAWN EOS multiangle laser light scattering detector (690 nm) were employed in the analysis. The d*n*/d*c* of P(AMPS) (0.181 mL/g) and P(AMPS-*b*-AAL) (0.170 mL/g) in the ASEC eluent were determined at 35 °C. The absolute molecular weights and polydispersities of PDMAPA and PDMAEMA were determined by ASEC using SynChropak CATSEC columns (100, 300, and 1000 Å; Eichrom Technologies Inc.), a Wyatt Optilab DSP interferometric refractometer, a Wyatt DAWN DSP multiangle laser light scattering detector (λ = 690 nm), and 1 wt % acetic acid/0.1 M Na_2SO_4(aq) as the eluent at a flow rate of 0.25 mL/min. The d*n*/d*c* of PDMAPA (0.163 mL/g) and PDMAEMA (0.160 mL/g) in the cationic eluent were determined at 35 °C.

NMR spectra were recorded in D_2O using a Mercury Innova 500 MHz spectrometer. Solution pD was adjusted using either DCl or NaOD.

Dynamic light scattering measurements were conducted on the block copolymer series at a concentration of 1.0 g/L in aqueous solution using a Malvern Instruments Zetasizer Nano ZS series instrument equipped with a 4 mW He−Ne laser operating at λ = 632.8 nm at an angle of 173°, an avalanche photodiode detector with high quantum efficiency, and an ALV/LSE-5003 multiple τ digital correlator electronics system. Dispersion Technology Software 5.03 (Malvern Instruments) was used to record and analyze the data to determine particle size distributions.

Variable-angle DLS and SLS measurements were made using incident light at 633 nm from a Spectra Physics HeNe operating at 40 mW. The angular dependence of the autocorrelation functions was measured using a Brookhaven Instruments BI-200SM goniometer with an avalanche photodiode detector and TurboCorr correlator. Correlation functions were analyzed according to the method of cumulants using the companion software. All data reported correspond to the average decay rate obtained from the second cumulant fit. Apparent diffusion coefficients (D_{app}) were obtained from the slope of the relaxation frequency (Γ) vs q^2 where

$$q = \frac{4\pi n}{\lambda}\sin\left(\frac{\theta}{2}\right) \quad (1)$$

λ is the wavelength of the incident laser (633 nm), θ is the scattering angle, and n is the refractive index of the media. The hydrodynamic radius (R_h) was then calculated from the Stokes−Einstein equation

$$R_h = \frac{k_B T}{6\pi\eta D_{app}} \quad (2)$$

where k_B is the Boltzmann constant, T is the temperature, and η is the viscosity of the medium.

Angular-dependent static light scattering (SLS) experiments were performed on aqueous polymer solutions with the same instrument as described above. The radius of gyration (R_g) of the assemblies was determined from the angular dependence of the scattering intensity. A Zimm plot of the scattering intensity (I_{ex}) versus the square of the scattering vector (q) was used to determine the radius of gyration (R_g). A Berry plot ($I_{ex}^{-1/2}$ vs q^2) is used in instances where a Zimm treatment results in upward curvature of the data when $qR_g \geq 1$.

Solutions for SLS experiments were prepared by dissolving the polymer in purified water at a concentration of 0.01 wt %. Samples were agitated to ensure complete dissolution and then filtered through a 0.45 μm PVDF syringe-driven filter (Millipore) directly into the scattering cell. Samples were then sonicated and allowed to reach thermal equilibrium prior to measurements.

Transmission electron microscopy (TEM) measurements were conducted using a JEOL JEM-2100 electron microscope at an acceleration voltage of 200 kV. Samples were prepared by placing a 5 μL drop of the 0.1 wt % nanoparticle solution on a Formvar-coated copper grid followed by water evaporation in an incubator at 45 °C.

Atomic force microscopy (AFM) imaging was performed with a Veeco Dimension 3000 AFM (Veeco Instruments Inc.). Morphologies were investigated in tapping mode operation in air. A RTSP silicon cantilever (Veeco Probes, Santa Barbara, CA) was used for dry imaging. Samples were prepared by placing a 5 μL drop of the 0.1 wt % nanoparticle solution on a neat silicon wafer followed by water evaporation at room temperature.

General Procedure for the RAFT Polymerization of AMPS. RAFT-mediated polymerizations of AMPS were conducted at 70 °C, employing V-501 as the primary radical source and CTP as the RAFT chain transfer agent (CTA). Polymerizations were performed directly in water (pH 6.5) with an initial monomer concentration ($[M]_0$) of 1.0 M under a nitrogen atmosphere in round-bottom flasks equipped with magnetic stir bars and sealed with rubber septa. The $[M]_0$:$[CTA]_0$ was adjusted to yield polymers with the desired molecular weight at 30% conversion while the $[CTA]_0$:$[I]_0$ was 5:1. The conversion was kept low to maintain control and prevent loss of the CTA end group for further blocking. For example, AMPS (13.1 g, 63.1 mmol), CTP (56.3 mg, 0.2 mmol), and V-501 (11.3 mg, 0.04 mmol) were added along with deionized (DI) water (65 mL) to a round-bottom flask, and the solution pH was adjusted to 6.5. After purging with nitrogen for 30 min, the polymerization was allowed to proceed at 70 °C for 2 h. The reaction was terminated by cooling the reaction flask in liquid nitrogen followed by exposure to air. The products were purified by dialysis against DI water for 3 days and isolated by lyophilization. The structural data of the resulting macro-CTAs are shown in Table 1 while the GPC chromatograms are shown in the Supporting Information (Figures S1 and S2).

Block Copolymer Synthesis. A PAMPS macro-CTA was utilized in the preparation of diblock copolymers P(AMPS$_n$-*b*-AAL$_m$). Polymerizations were performed directly in water

Table 1. Molecular Weight (M_n), Polydispersity Index (PDI), and AMPS/AAL Weight Percents for P(AMPS$_n$-*b*-AAL$_m$) Block Copolymers

polymer[a]	M_n (kDa)[b]	PDI[b]	AMPS/ALAla (wt %)
P(AMPS$_{110}$)	25.1	1.10	100/0
P(AMPS$_{110}$-*b*-AAL$_{185}$)	51.8	1.23	48/52
P(AMPS$_{110}$-*b*-AAL$_{305}$)	68.7	1.27	36/64
P(AMPS$_{110}$-*b*-AAL$_{490}$)	95.1	1.23	26/74
P(AMPS$_{225}$)	51.4	1.14	100/0
P(AMPS$_{225}$-*b*-AAL$_{350}$)	101.3	1.22	51/49
P(AMPS$_{225}$-*b*-AAL$_{660}$)	145.9	1.26	35/65
P(AMPS$_{225}$-*b*-AAL$_{1000}$)	198.4	1.29	26/74

[a] Subscripts represent the degree of polymerization (DP) for the respective blocks. [b] As determined by aqueous size exclusion chromatography (ASEC).

(pH 6.5) with $[M]_0$ equal to 1.0 M under a nitrogen atmosphere in round-bottom flasks equipped with magnetic stir bars and sealed with rubber septa. The $[M]_0$:$[CTA]_0$ was adjusted to yield polymers with the desired molecular weight at 60% conversion while the initial $[CTA]_0$:$[I]_0$ was 5:1. For example, P(AMPS$_{225}$-*b*-AAL$_{350}$) was prepared by adding PAMPS$_{225}$ macro-CTA (1.23 g, 0.024 mmol), AAL (2.00 g, 14.0 mmol), and V-501 (1.3 mg, 0.005 mmol) along with deionized (DI) water (14 mL) to a round-bottom flask, and the solution pH was adjusted to 6.5. After sparging with nitrogen for 30 min, the polymerization was allowed to proceed at 70 °C for 5.5 h. The reaction was terminated by cooling the reaction flask in liquid nitrogen followed by exposure to air. The products were purified by dialysis against DI water for 3 days and isolated by lyophilization. The structural data of the resulting block copolymers are shown in Table 1 while the GPC chromatograms are shown in the Supporting Information (Figures S1 and S2).

Preparation and Interpolyelectrolyte Complexation of Micelles. Copolymers were dissolved directly in HPLC grade water (1 mg/mL). Micellization was achieved by adjusting the pH of the solution to 1.0 using 1 M HCl. Shell cross-linked micelles were prepared from an aqueous solution of the copolymer (0.5 mg/mL, pH 1.0). An aqueous solution of either PDMAPA (M_n = 155 500 Da, PDI = 1.06) or PDMAEMA (M_n = 25 200 Da, PDI = 1.11) (0.5 mg/mL) was adjusted to pH 1.0 and added slowly (0.05 mL/min) to a final mole ratio of AMPS:cationic repeat unit of 4:1 and allowed to stir for an hour.

Results and Discussion

In this work, we sought to combine the stimuli-responsive behavior of a doubly hydrophilic polyanionic diblock copolymer and interpolyelectrolyte complex (IPEC) formation to prepare "locked" nanoscale micellar assemblies which could readily dissociate with changes in pH. For our structural diblock design, we chose a hydrophilic, anionically charged PAMPS block and a pH-responsive PAAL block with respective pK_a values of < 2 and 3.5. By utilizing appropriate RAFT polymerization conditions, a range of well-defined blocks and compositions are available.[3,45] PAMPS was chosen due to its permanent hydrophilicity over the pH range studied while PAAL was chosen in order to exploit the hydrophilic to hydrophobic transition which occurs at low pH values. The two cationic homopolymers, PDMAPA and PDMAEMA, were chosen for subsequent IPEC formation with block copolymer micelles to demonstrate the tunability of their dissociation. The demonstrated reversibility of these systems suggest future application of the IPEC micelles as drug delivery vehicles.

RAFT Synthesis of P(AMPS-*b*-AAL). We utilized aqueous RAFT polymerization conditions to synthesize the pH-responsive block copolymers, P(AMPS$_n$-*b*-AAL$_m$), as detailed in the Experimental Section and shown in Scheme 1.

Scheme 1. Synthetic Pathway for the Preparation of P(AMPS$_n$-*b*-AAL$_m$) Block Copolymers via Aqueous RAFT Polymerization

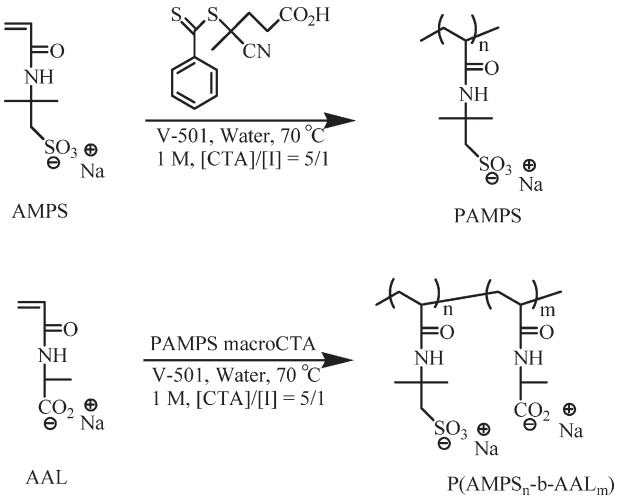

Scheme 2. Micelle Formation, Shell Cross-Linking, Solvation of the PAAL Block, and Dissociation of Shell Cross-Linked Assembly

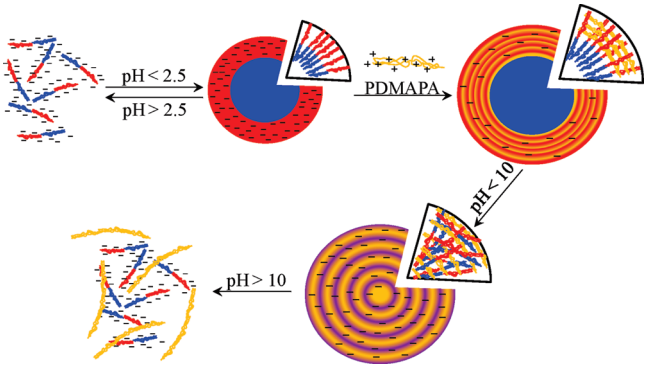

Two PAMPS macro-CTAs with targeted degrees of polymerization (DPs) of 100 and 200 were first prepared by employing CTP to control the polymerization at 70 °C, using V-501 as the primary radical source. The solution pH was kept at 6.5 in order to reduce CTA hydrolysis.[46] The two PAMPS macro-CTAs had number-average molecular weight (M_n) and polydispersity index (PDI) values of 25 100 Da (1.10) and 51 400 Da (1.14), respectively. These macro-CTAs were subsequently utilized to prepare block copolymers with AAL weight fractions of 0.75, 0.65, and 0.50. The polymerization time was kept constant while the $[M]_0$:$[CTA]_0$ was adjusted to yield block copolymers with the desired lengths. Aqueous size exclusion chromatography with multiangle laser light scattering (ASEC-MALLS) was used to determine M_n and PDI data shown in Table 1. Under the given conditions, well-defined diblock copolymers with unimodal ASEC chromatograms and relatively low PDIs (< 1.30) were obtained, indicating that the polymerizations proceeded in a controlled manner (see Figures S1 and S2 in the Supporting Information). Selected polymers were then used in experiments to demonstrate first pH-responsive formation of nanostructures and then reversible interpolyelectrolyte shell cross-linking of those structures (Scheme 2).

Self-Assembly Behavior of P(AMPS-*b*-AAL). The self-assembly behavior of the block copolymers was followed by dynamic light scattering (DLS). Below the pK_a of PAAL (3.5), segments are protonated, rendering them hydrophobic and leading to self-assembly. PAMPS, a strong polyacid,

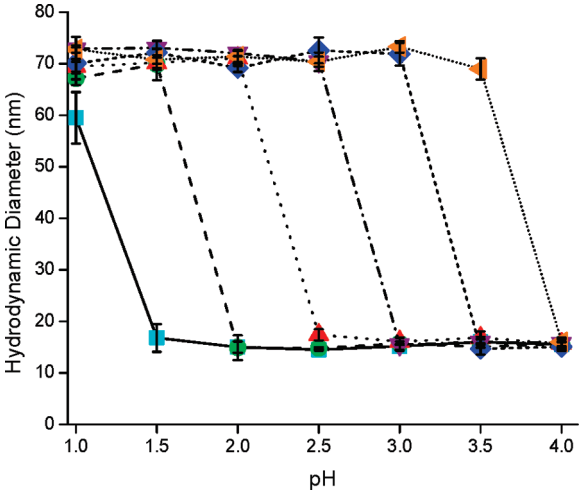

Figure 1. Hydrodynamic diameter versus solution pH for a 0.1 wt % P(AMPS$_{110}$-*b*-AAL$_{490}$) solution at salt concentrations of 0 (■), 0.05 (●), 0.15 (▲), 0.3 (▼), 0.8 (◆), and 1.4 M NaCl (tilted ▲). Lines are used to guide the eye.

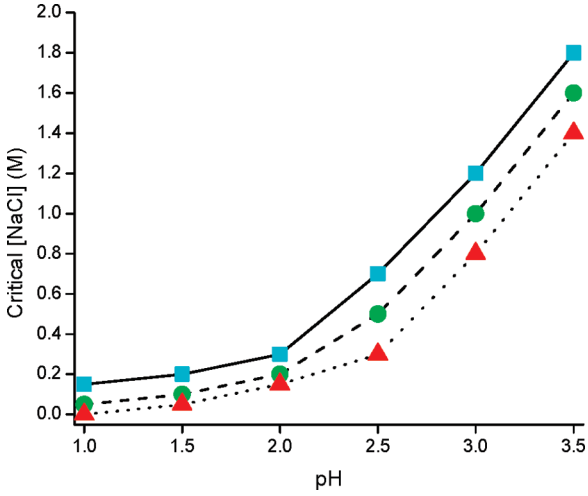

Figure 2. Critical salt concentration (CSC) required for the formation of micelles as a function of pH as determined from dynamic light scattering for P(AMPS$_{110}$-*b*-AAL$_{185}$) (■), P(AMPS$_{110}$-*b*-AAL$_{305}$) (●), and P(AMPS$_{110}$-*b*-AAL$_{490}$) (▲). Lines are used to guide the eye.

which remains negatively charged even at extremely low pH values and high salt concentrations, is permanently hydrophilic across the pH and salt concentrations utilized in this research. As such, the block copolymers P(AMPS$_n$-*b*-AAL$_m$) are expected to form AAL-core and AMPS-shell micelles when the solution pH is lowered below the pK_a of PAAL. However, the block copolymers did not form aggregates around the pK_a of the PAAL block in water at ambient conditions. After further investigation, it was determined that aggregation could be induced by further lowering the pH to protonate the entire PAAL block (pH = 1) or by adding small molecule electrolytes at pH values ≤3.5. It is reasoned that the addition of salt promotes assembly by screening the charges of the PAMPS and any unprotonated carboxylic acids on the PAAL. Similar results have been previously reported by Armes and co-workers[47] for PDMAEMA/PDEAEMA block copolymers.

The aggregation behavior of the block copolymer series synthesized from the PAMPS$_{110}$ macro-CTA was studied utilizing DLS. For these studies the solution pH values were varied from 4.0 to 1.0 in 0.5 increments. Given the salt-dependent assembly, the electrolyte concentration was also varied in order to determine the critical salt concentration (CSC) necessary for the formation of micelles at specific solution pH values. Figure 1 shows the hydrodynamic diameter of P(AMPS$_{110}$-*b*-AAL$_{490}$) at designated pH and salt concentrations. When no electrolyte is present, the block copolymers remain unimers in solution (~15 nm) above pH 1.0; however, at pH 1.0 the block copolymers aggregate into micelles with average hydrodynamic diameters of about 60 nm, apparently from maximum protonation of carboxylic acid groups and sufficient ionic strength. By adding salt to promote the screening of the charged units, aggregation can be induced at higher pH values. As shown in Figure 1, as pH increases, so does the ionic strength required for micelle formation. At a salt concentration of 1.4 M, micelles are formed at pH 3.5 (the pK_a of the PAAL block). Similar results were obtained for P(AMPS$_{110}$-*b*-AAL$_{185}$) and P(AMPS$_{110}$-*b*-AAL$_{305}$) (see Figures S3 and S4 in the Supporting Information).

Figure 2 shows a plot of the CSC required for micelle formation as a function of solution pH for P(AMPS$_{110}$-*b*-AAL$_{185}$), P(AMPS$_{110}$-*b*-AAL$_{305}$), and P(AMPS$_{110}$-*b*-AAL$_{490}$). By maintaining a constant PAMPS block length, the effect of the PAAL block length on self-assembly can be determined. As demonstrated in the figure, increasing the PAAL block length leads to a decrease in the CSC required for micelle formation at a specific pH value. Although the percentage of protonated PAAL units remains the same for each block copolymer at a specific pH value, the overall hydrophobicity of the polymers increases as the PAAL block length increases. Therefore, stable micelles form, requiring less charge screening from added electrolyte. It is interesting to note that increasing the NIPAM block length in thermally responsive block copolymers lowers the critical temperature for micelle formation in a similar fashion.[48,49] In both cases the effective length of the induced hydrophobe segment controls the unimer-to-micelle transition.

The same experiments were performed with a series of block copolymers synthesized utilizing the PAMPS$_{225}$ macro-CTA in order to validate the results from the previous study. Figure 3 shows a plot of the hydrodynamic diameter of P(AMPS$_{225}$-*b*-AAL$_{1000}$) as a function of pH at varying salt concentrations. It is interesting to note that when no salt is present, the block copolymer can form micelles at pH values up to 2.0 whereas P(AMPS$_{110}$-*b*-AAL$_{490}$) requires a pH of 1.0 for aggregation to occur. Even though these two block copolymers have the same weight percent AAL (75 wt %), aggregation occurs under different solution conditions, which suggests that the aggregation more strongly depends on the block length of the responsive segment rather than its overall weight percent in the block copolymer. The aggregation behavior of P(AMPS$_{225}$-*b*-AAL$_{350}$) and P(AMPS$_{225}$-*b*-AAL$_{660}$) was also examined and is shown in Figures S5 and S6 of the Supporting Information. A plot of the CSC necessary for micelle formation as a function of solution pH for this series of block copolymers is shown in Figure 4. Similar to the behavior of the PAMPS$_{110}$ block copolymer series, the CSC at a specific pH decreases as the block length of AAL increases.

In order to determine the structural properties of these block copolymers, dynamic light scattering (DLS) and static light scattering (SLS) were used to determine the hydrodynamic radii (R_h) and radii of gyration (R_g), respectively. The ratio of R_g to R_h, or ρ, is known as the shape factor, with spherical micelles having values of ~0.775.[50] The experimental values of R_g, R_h, and R_g/R_h for all block copolymers in this study are shown in Table 2. As determined by DLS, the hydrodynamic radii for P(AMPS$_{110}$-*b*-AAL$_{185}$), P(AMPS$_{110}$-*b*-AAL$_{305}$), and P(AMPS$_{110}$-*b*-AAL$_{490}$) increase as the AAL block length

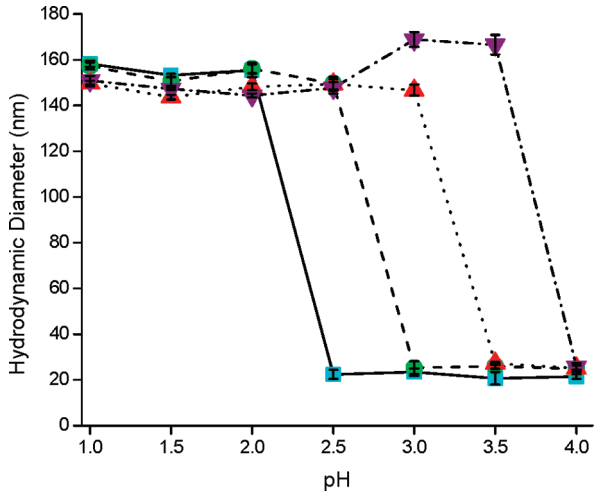

Figure 3. Hydrodynamic diameter versus solution pH for a 0.1 wt % P(AMPS$_{225}$-*b*-AAL$_{1000}$) solution at salt concentrations of 0 (■), 0.1 (●), 0.6 (▲), and 1.4 M NaCl (▼). Lines are used to guide the eye.

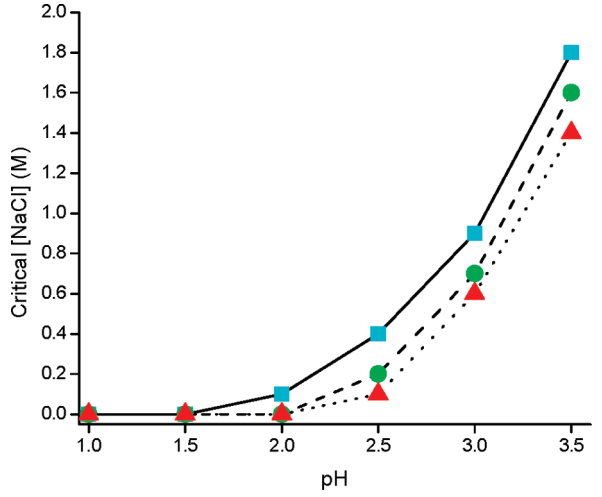

Figure 4. Critical salt concentration (CSC) required for the formation of micelles as a function of pH measured by dynamic light scattering for P(AMPS$_{225}$-*b*-AAL$_{350}$) (■), P(AMPS$_{225}$-*b*-AAL$_{660}$) (●), and P(AMPS$_{225}$-*b*-AAL$_{1000}$) (▲). Lines are used to guide the eye.

increases. The same trend is observed for the block copolymer series derived from PAMPS$_{225}$. These results are consistent with previous results from our lab[51] and from Perrier's research group.[48] In order to better understand the morphology of these aggregates in solution, SLS was utilized to obtain the R_g. As shown in Table 2, the shape factors are close to the predicted value for spherical micelles.

Transmission electron microscopy (TEM) and atomic force microscopy (AFM) were used as complementary means to determine the morphological properties. Figure 5 shows the TEM and AFM images of the micelles formed at pH 1.0. Both techniques confirm the spherical nature of the micelles and reveal radii of approximately 25 and 27 nm, respectively. These values are lower than those observed by DLS (45 nm), which is consistent with the literature reports of dehydration during sample measurement in both TEM[16,52] and AFM.[53,54] Sizes determined from AFM and TEM images are in good agreement.

Interpolyelectrolyte Cross-Linking. The anionic corona of the block copolymer micelles can be utilized for formation of interpolyelectrolyte complexes (IPECs) using cationic polymers with different pK_a values. In turn, the cross-linked micelles

Table 2. Radius of Gyration (R_g), Hydrodynamic Radius (R_h), and R_g/R_h for P(AMPS$_n$-*b*-AAL$_m$) Block Copolymers

polymer	radius of gyration (R_g) (nm)[a]	hydrodynamic radius (R_h) (nm)[b]	R_g/R_h
P(AMPS$_{110}$-*b*-AAL$_{185}$)	19[c]	27[c]	0.72
P(AMPS$_{110}$-*b*-AAL$_{305}$)	23[c]	29[c]	0.78
P(AMPS$_{110}$-*b*-AAL$_{490}$)	26[c]	35[c]	0.77
P(AMPS$_{225}$-*b*-AAL$_{350}$)	31	43	0.72
P(AMPS$_{225}$-*b*-AAL$_{660}$)	35	45	0.77
P(AMPS$_{225}$-*b*-AAL$_{1000}$)	41	70	0.59

[a] As determined by static light scattering (SLS) in solution at pH 1. [b] As determined by dynamic light scattering (DLS) in solution at pH 1. [c] As determined in solution at pH 1 and 0.2 M NaCl.

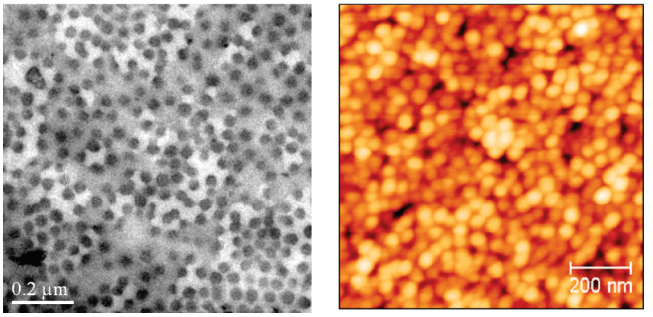

Figure 5. Transmission electron microscopy (left) and atomic force microscopy (right) images of micelles assembled from P(AMPS$_{225}$-*b*-AAL$_{660}$).

should exhibit pH-dependent reversibility. To illustrate, we chose cationic homopolymers, PDMAPA and PDMAEMA, with respective pK_a values of 8.5, determined experimentally (data not shown), and 7.3.[35] Micelles assembled at low pH using P(AMPS$_{225}$-*b*-AAL$_{1000}$) were ionically cross-linked with these cationic polymers as outlined in Scheme 2. From the Zimm plot (Figure S8) and the molecular weight of the polymer, an aggregation number for the self-assembled micelles of this block copolymer was calculated to be 330. Because of this large aggregation number, a 4:1 mole ratio of AMPS:cationic repeat unit was used to form the interpolyelectrolyte complexes (IPECs), ensuring that sufficient residual anionic charges are present on the micelles to prevent aggregation of the soluble complexes.

The reversibility of this IPEC cross-linked micelle was studied utilizing ^{1}H NMR[41,51,55,56] under specified conditions as illustrated in Figure 6. Spectra (i) and (ii) are of molecularly dissolved PDMAEMA and P(AMPS$_{225}$-*b*-AAL$_{350}$) at pD 7.0. Upon decreasing the pD to 1.0 with DCl (iii), signals from the methyl "c" and methine "d" groups of PAAL are broadened relative to those associated with PAMPS. After cross-linking with PDMAEMA at pD 1.0 (iv), the methyl and methylene signals associated with PAMPS, peaks "a" and "b", decreases due to reduced mobility caused by the cross-linking. Also, the methyl signal "e" from PDMAEMA appears at to 2.96 ppm due to the interaction of the amine and sulfonate groups. After increasing the pD to 7.0 using NaOD (v), an increase in the intensity of the methyl proton "c" associated with PAAL is observed due to the solubility of the PAAL block at this pD. Also, the methyl proton "e" remains shifted, indicating that the micelles are still cross-linked. Further increasing the pD to 9.0 (vi) results in dissociation of the IPEC, and all peaks associated with both the block copolymer and the cationic polymer are observed at their neutral locations.

The reversibility of the cross-linking of these micelles was also followed by DLS under specified conditions. Figure 7 shows the aggregation behavior when PDMAPA is used as

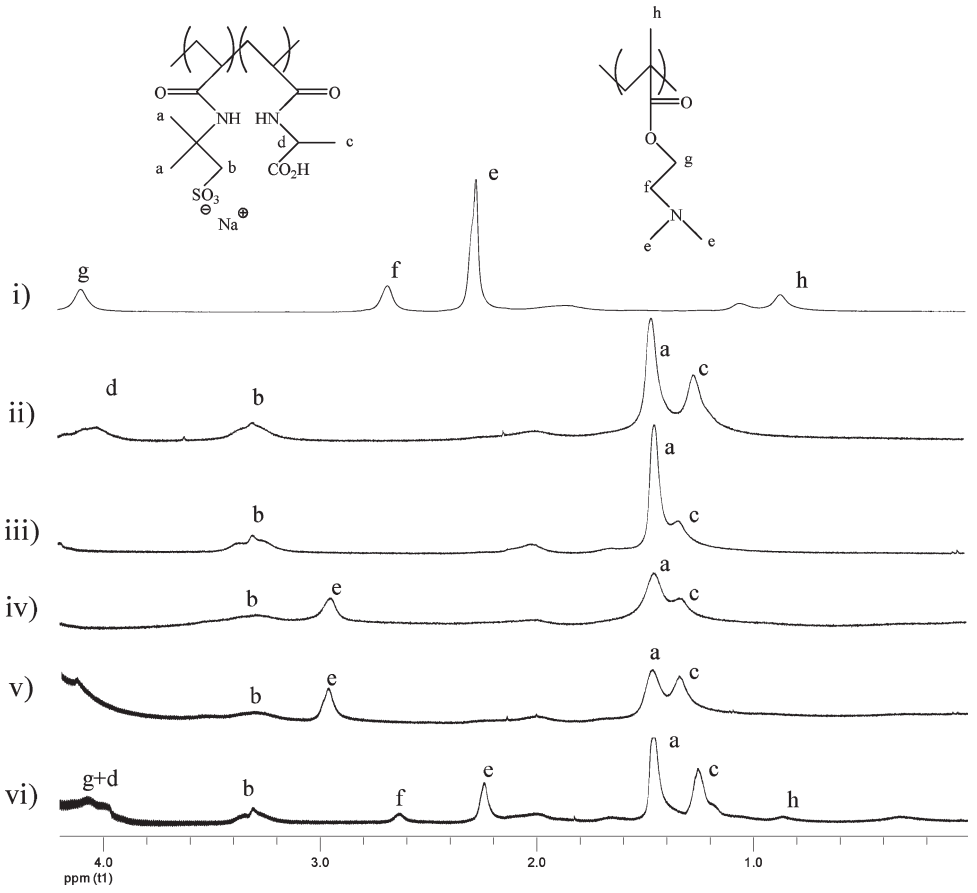

Figure 6. ^{1}H NMR spectra for PDMAEMA$_{160}$ complexation with the block copolymer P(AMPS$_{225}$-*b*-AAL$_{350}$): PDMAEMA$_{160}$ at pD 7.0 (i), P(AMPS$_{225}$-*b*-AAL$_{350}$) at pD 7.0 (ii), P(AMPS$_{225}$-*b*-AAL$_{350}$) at pD 1.0 (iii), P(AMPS$_{225}$-*b*-AAL$_{350}$) after formation of interpolyelectrolyte complex with PDMAEMA$_{160}$ at pD 1.0 (iv), P(AMPS$_{225}$-*b*-AAL$_{350}$) after formation of interpolyelectrolyte complex with PDMAEMA$_{160}$ at pD 7.0 (v), and P(AMPS$_{225}$-*b*-AAL$_{350}$) and PDMAEMA$_{160}$ after increasing the pD to 9.0 (vi).

the cationic cross-linker. At pH 7.0, P(AMPS$_{225}$-*b*-AAL$_{1000}$) copolymers exist as unimers with an apparent hydrodynamic diameter (D_h) of 25 nm (Figure 7, peak A). When the solution pH is lowered to 1.0, the polymers assemble into micelles with an average apparent D_h of 150 nm (Figure 7, peak B). The addition of PDMAPA leads to interpolyelectrolyte complexed micelles with an apparent D_h value of 190 nm (Figure 7, peak C). Similar results showing an increase in size of IPEC micelles have also been reported by Armes et al.[41] "Locking" of the nanoparticle is demonstrated by increasing the pH of the solution to 9.0 where un-cross-linked P(AMPS$_{225}$-*b*-AAL$_{1000}$) would dissociate to unimers; however, under these conditions only micelles with an average apparent D_h of 300 nm are observed by DLS (Figure 7, peak D). This increase in diameter is due to the PAAL block becoming soluble leading to "swollen" micelle structures. Dissociation of the IPECs is induced by further increasing the solution pH to 10.0 fully deprotonating PDMAPA. Upon removal of the cationic charge, the interpolyelectrolyte complex dissociates to form unimers of 28 nm (Figure 7, peak E). Further detail of the cross-linked micelle size versus pH can be found in Figure S9 of the Supporting Information.

In order to demonstrate the tunability of reversible shell cross-linking, PDMAEMA (pK_a = 7.3) was utilized as a cross-linker. Given the lower pK_a of PDMAEMA compared to PDMAPA, dissociation should occur at a lower pH value. Figure 8 shows the size distributions at varying conditions. After cross-linking with PDMAEMA an increase in the D_h value to 190 nm was observed (Figure 8, peak C). Upon

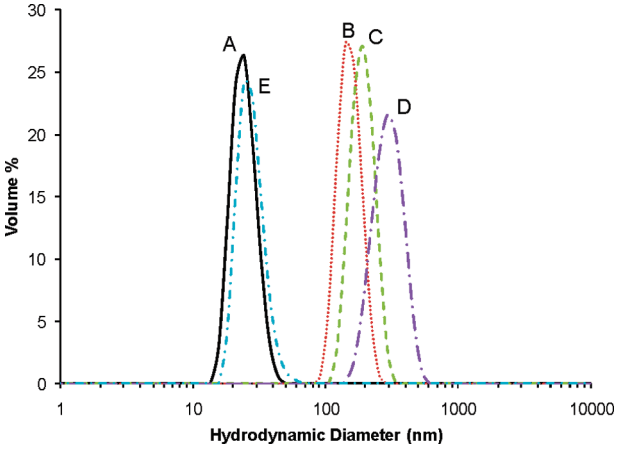

Figure 7. Size distribution (measured by dynamic light scattering) of P(AMPS$_{225}$-*b*-AAL$_{1000}$): pH 7.0 (A), pH 1.0 (B), after formation of interpolyelectrolyte complex (IPEC) at pH 1.0 (C), IPEC at pH 9.0 (D), dissociated IPEC at pH 10.0 (E).

increasing the pH to 7.0 after IPEC formation, the micelles remained intact with an apparent D_h value of 300 nm (Figure 8, peak D). Again, the micelle sizes increase due to the PAAL block becoming soluble. By further increasing the pH to 9.0, the IPEC dissociates to unimers of 28 nm (Figure 8, peak E). Further detail of the cross-linked micelle size versus pH can be found in Figure S10 of the Supporting Information. With the cationic polymer PDMAPA, the

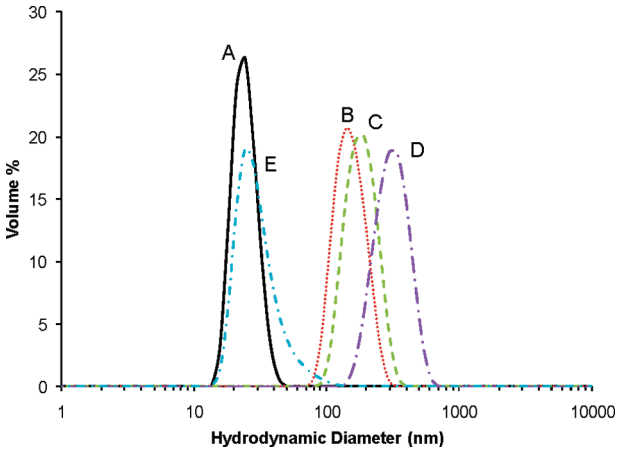

Figure 8. Size distribution (measured by dynamic light scattering) of P(AMPS$_{225}$-*b*-AAL$_{1000}$): pH 7.0 (A), pH 1.0 (B), after formation of interpolyelectrolyte complex (IPEC) at pH 1.0 (C), IPEC at pH 7.0 (D), dissociated IPEC at pH 9.0 (E).

complexes remain cross-linked at pH 9.0 because a significant number of cationic charges still remain, preventing dissociation. By contrast, the pK_a of PDMAEMA is significantly lower than that of PDMAPA, and thus there are insufficient charges to maintain the complexes at this pH. These results provide further evidence that the nature of the cationic cross-linker directly affects the pH-dependent dissociation of the IPECs.

Conclusions

A series of block copolymers composed of AMPS and AAL with varying block lengths had been synthesized. The weight percent of amphiphilic AAL in the block copolymers was varied, and the effect on pH-responsive assembly was observed. The self-assembly behavior of these copolymers was determined over a range of pH values and salt concentrations. By plotting the critical salt concentration necessary for micelle formation versus solution pH, we observed that increasing the AAL block length leads to a lower CSC which is attributed to an overall higher percent of hydrophobicity within the block copolymer. DLS and SLS studies were utilized to determine the nature of the aggregates formed by the block copolymers. TEM and AFM were then used to confirm the sizes of self-assembled micelles. The cationic homopolymers PDMAPA and PDMAEMA were employed for the *in situ* formation of corona cross-linked micelles via interpolyelectrolyte complexation. DLS and ^{1}H NMR spectroscopy indicate the micelles are stable, yet reversible with changes in pH. The ionically cross-linked micelles were shown to dissociate at pH values above the pK_a of the cationic polymer. This system may have utility over traditional covalent methodologies based on the ease of synthesis and cross-linking, the interpolyelectrolyte cross-linked micelle reversibility, and the tunable control of the pH at which these cross-linked micelles dissociate.

Acknowledgment. The authors thank the MRSEC program of the National Science Foundation (DMR-0213883) and the Department of Energy (DE-FC26-01BC15317) for financial support. The authors acknowledge the NSF Division of Materials Research/Major Research Instrumentation Awards 0079450 and 0421406 for the purchase of the Varian Unity Inova 500 MHz NMR spectrometer and JEOL JEM-2100 electron microscope. The authors also thank Dr. Sarah E. Morgan and Chris Harris for their assistance in AFM analysis. Wako Chemicals is also acknowledged for donating the diazo initiator V-501.

Supporting Information Available: Experimental details, size exclusion chromatography, and static and dynamic light scattering. This material is available free of charge via the Internet at http://pubs.acs.org.

References and Notes

(1) Andre, X.; Zhang, M. F.; Muller, A. H. E. *Macromol. Rapid Commun.* **2005**, *26*, 558–563.
(2) Colfen, H. *Macromol. Rapid Commun.* **2001**, *22*, 219–252.
(3) Lokitz, B. S.; Convertine, A. J.; Ezell, R. G.; Heidenreich, A.; Li, Y.; McCormick, C. L. *Macromolecules* **2006**, *39*, 8594–8602.
(4) Riess, G. *Prog. Polym. Sci.* **2003**, *28*, 1107–1170.
(5) Rodriguez-Hernandez, J.; Babin, J.; Zappone, B.; Lecommandoux, S. *Biomacromolecules* **2005**, *6*, 2213–2220.
(6) Rodriguez-Hernandez, J.; Checot, F.; Gnanou, Y.; Lecommandoux, S. *Prog. Polym. Sci.* **2005**, *30*, 691–724.
(7) Wooley, K. L. *J. Polym. Sci., Part A: Polym. Chem.* **2000**, *38*, 1397–1407.
(8) Thurmond, K. B.; Kowalewski, T.; Wooley, K. L. *J. Am. Chem. Soc.* **1997**, *119*, 6656–6665.
(9) Huang, H.; Remsen, E. E.; Wooley, K. L. *Chem. Commun.* **1998**, 1415–1416.
(10) Huang, H.; Remsen, E. E.; Kowalewski, T.; Wooley, K. L. *J. Am. Chem. Soc.* **1999**, *121*, 3805–3806.
(11) Ma, Q.; Wooley, K. L. *J. Polym. Sci., Part A: Polym. Chem.* **2000**, *38*, 4805–4820.
(12) Ma, Q.; Remsen, E. E.; Kowalewski, T.; Wooley, K. L. *J. Am. Chem. Soc.* **2001**, *123*, 4627–4628.
(13) Underhill, R. S.; Liu, G. *Chem. Mater.* **2000**, *12*, 2082–2091.
(14) Becker, M. L.; Remsen, E. E.; Wooley, K. L. *J. Polym. Sci., Part A: Polym. Chem.* **2001**, *39*, 4152–4166.
(15) Fujii, S.; Cai, Y.; Weaver, J. V. M.; Armes, S. P. *J. Am. Chem. Soc.* **2005**, *127*, 7304–7305.
(16) Butun, V.; Wang, X. S.; de PazBanez, M. V.; Robinson, K. L.; Billingham, N. C.; Armes, S. P.; Tuzar, Z. *Macromolecules* **2000**, *33*, 1–3.
(17) Luo, L.; Eisenberg, A. *Angew. Chem., Int. Ed.* **2002**, *41*, 1001–1004.
(18) Liu, S.; Armes, S. P. *J. Am. Chem. Soc.* **2001**, *123*, 9910–9911.
(19) Zhang, L.; Eisenberg, A. *Science* **1995**, *268*, 1728–1731.
(20) Sanji, T.; Nakatsuka, Y.; Kitayama, F.; Sakurai, H. *Chem. Commun.* **1999**, 2201–2202.
(21) Sanji, T.; Nakatsuka, Y.; Ohnishi, S.; Sakurai, H. *Macromolecules* **2000**, *33*, 8524–8526.
(22) Thurmond, K. B.; Kowalewski, T.; Wooley, K. L. *J. Am. Chem. Soc.* **1996**, *118*, 7239–7240.
(23) Ding, J.; Liu, G. *Macromolecules* **1998**, *31*, 6554–6558.
(24) Stewart, S.; Liu, G. *Chem. Mater.* **1999**, *11*, 1048–1054.
(25) Jiang, X.; Luo, S.; Armes, S. P.; Shi, W.; Liu, S. *Macromolecules* **2006**, *39*, 5987–5994.
(26) Huang, H.; Kowalewski, T.; Remsen, E. E.; Gertzmann, R.; Wooley, K. L. *J. Am. Chem. Soc.* **1997**, *119*, 11653–11659.
(27) Zhang, Q.; Remsen, E. E.; Wooley, K. L. *J. Am. Chem. Soc.* **2000**, *122*, 3642–3651.
(28) Butun, V.; Billingham, N. C.; Armes, S. P. *J. Am. Chem. Soc.* **1998**, *120*, 12135–12136.
(29) Butun, V.; Lowe, A. B.; Billingham, N. C.; Armes, S. P. *J. Am. Chem. Soc.* **1999**, *121*, 4288–4289.
(30) Liu, S.; Weaver, J. V. M.; Tang, Y.; Billingham, N. C.; Armes, S. P.; Tribe, K. *Macromolecules* **2002**, *35*, 6121–6131.
(31) Liu, S.; Ma, Y.; Armes, S. P.; Perruchot, C.; Watts, J. F. *Langmuir* **2002**, *18*, 7780–7784.
(32) Liu, S.; Weaver, J. V. M.; Save, M.; Armes, S. P. *Langmuir* **2002**, *18*, 8350–8357.
(33) Joralemon, M. J.; O'Reilly, R. K.; Hawker, C. J.; Wooley, K. L. *J. Am. Chem. Soc.* **2005**, *127*, 16892–16899.
(34) Li, Y.; Smith, A. E.; Lokitz, B. S.; McCormick, C. L. *Macromolecules* **2007**, *40*, 8524–8526.
(35) Smith, A. E.; Xu, X.; Abell, T. U.; Kirkland, S. E.; Hensarling, R. M.; McCormick, C. L. *Macromolecules* **2009**, *42*, 2958–2964.
(36) Li, Y.; Lokitz, B. S.; Armes, S. P.; McCormick, C. L. *Macromolecules* **2006**, *39*, 2726–2728.
(37) Li, Y.; Lokitz, B. S.; McCormick, C. L. *Macromolecules* **2006**, *39*, 81–89.
(38) Xu, X.; Smith, A. E.; Kirkland, S. E.; McCormick, C. L. *Macromolecules* **2008**, *41*, 8429–8435.

(39) Xu, X.; Smith, A. E.; McCormick, C. L. *Aust. J. Chem.* **2009**, *62*, 1520–1527.
(40) Read, E. S.; Armes, S. P. *Chem. Commun.* **2007**, 3021.
(41) Weaver, J. V. M.; Tang, Y.; Liu, S.; Iddon, P. D.; Grigg, R.; Armes, S. P.; Billingham, N. C.; Hunter, R.; Rannard, S. P. *Angew. Chem., Int. Ed.* **2004**, *43*, 1389–1392.
(42) Lokitz, B. S.; York, A. W.; Stempka, J. E.; Treat, N. D.; Li, Y.; Jarrett, W. L.; McCormick, C. L. *Macromolecules* **2007**, *40*, 6473–6480.
(43) Flores, J. D.; Xu, X.; Treat, N. J.; McCormick, C. L. *Macromolecules* **2009**, *42*, 4941–4945.
(44) Mitsukami, Y.; Donovan, M. S.; Lowe, A. B.; McCormick, C. L. *Macromolecules* **2001**, *34*, 2248–2256.
(45) Sumerlin, B. S.; Donovan, M. S.; Mitsukami, Y.; Lowe, A. B.; McCormick, C. L. *Macromolecules* **2001**, *34*, 6561–6564.
(46) Thomas, D. B.; Convertine, A. J.; Myrick, L. J.; Scales, C. W.; Smith, A. E.; Lowe, A. B.; Vasileva, Y. A.; McCormick, C. L. *Macromolecules* **2004**, *37*, 8941–8950.
(47) Lee, A. S.; Gast, A. P.; Bütün, V.; Armes, S. P. *Macromolecules* **1999**, *32*, 4302–4310.
(48) Liu, B.; Perrier, S. *J. Polym. Sci., Part A: Polym. Chem.* **2005**, *43*, 3643–3654.
(49) Xia, Y.; Yin, X.; Burke, N. A. D.; Stover, H. D. H. *Macromolecules* **2005**, *38*, 5937–5943.
(50) Burchard, W. *Adv. Polym. Sci.* **1983**, *48*, 1–124.
(51) Convertine, A. J.; Lokitz, B. S.; Vasileva, Y.; Myrick, L. J.; Scales, C. W.; Lowe, A. B.; McCormick, C. L. *Macromolecules* **2006**, *39*, 1724–1730.
(52) Resendes, R.; Massey, J.; Dorn, H.; Winnik, M. A.; Manners, I. *Macromolecules* **2000**, *33*, 8–10.
(53) Moughton, A. O.; Stubenrauch, K.; O'Reilly, R. K. *Soft Matter* **2009**, *5*, 2361–2370.
(54) Xie, M.; Kong, Y.; Han, H.; Shi, J.; Ding, L.; Song, C.; Zhang, Y. *React. Funct. Polym.* **2008**, *68*, 1601–1608.
(55) Sumerlin, B. S.; Lowe, A. B.; Thomas, D. B.; Convertine, A. J.; Donovan, M. S.; McCormick, C. L. *J. Polym. Sci., Part A: Polym. Chem.* **2004**, *42*, 1724–1734.
(56) Sumerlin, B. S.; Lowe, A. B.; Thomas, D. B.; McCormick, C. L. *Macromolecules* **2003**, *36*, 5982–5987.